

How Absorbed Hydrogen Affects Catalytic Activity of Transition Metals**

Hristiyan A. Aleksandrov, Sergey M. Kozlov, Svetlana Schaueremann,
Georgi N. Vayssilov, Konstantin M. Neymana

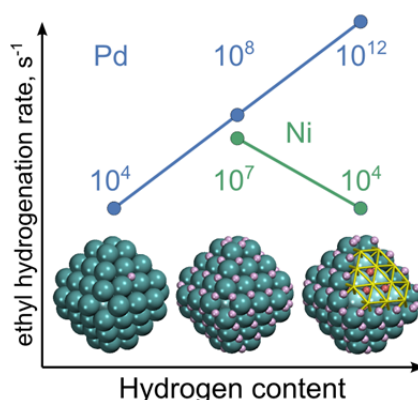


Table of Content graph

Subsurface hydrogen, H^{sub} , is shown to either increase or decrease significantly the bond energy and the reactivity of the adsorbed hydrogen, H^{ad} , depending on the metal. We calculate a representative reaction, ethyl hydrogenation, to speed up on Pd and Pt, but to slow down on Ni and Rh in the presence of H^{sub} , especially on metal nanoparticles. The reasons are *i*) occupation of antibonding H-Pd and H-Pt states and *ii*) electrostatic strengthening of polar H-Ni and H-Rh bonds by H^{sub} .

^[a] Dr. Hristiyan A. Aleksandrov, Sergey M. Kozlov, Prof. Dr. Konstantin M. Neyman

Departament de Química Física and Institut de Química Teòrica i Computacional (IQTUB), Universitat de Barcelona, Martí i Franquès 1, 08028 Barcelona, Spain

Dr. Hristiyan A. Aleksandrov, Prof. Dr. Georgi N. Vayssilov

Faculty of Chemistry and Pharmacy, University of Sofia, 1126 Sofia, Bulgaria

Dr. Svetlana Schaueremann

Department of Chemical Physics, Fritz-Haber-Institut der Max-Planck-Gesellschaft, 14195 Berlin, Germany

Prof. Dr. Konstantin M. Neyman

Institució Catalana de Recerca i Estudis Avançats (ICREA), 08010 Barcelona, Spain

Phone +34 93 40 37 212, Fax +34 93 40 21 231

E-mail: konstantin.neyman@icrea.cat

<http://www.icrea.cat/Web/ScientificForm.aspx?key=292>

^[**] The authors thank Prof. H.-J. Freund, Dr. S. Shaikhutdinov and Dr. L. V. Moskaleva for valuable discussions and critical reading of the manuscript. We acknowledge financial support provided by the EU (FP7-NMP.2012.1.1-1, project ref. N° 310191), the Spanish MINECO (grant CTQ2012-34969), MEDU (grants SB2010-0172 for H.A.A. and AP2009-3379 for S.M.K.) and Generalitat de Catalunya (grants 2014SGR97 and XRQTC). H.A.A. and G.N.V. are grateful to the Bulgarian Science Fund (grant DCVP 02/1) and the FP7 programme (project Beyond Everest). S.S. thanks the Verband der Chemischen Industrie for a Dozentenstipendium. We gratefully acknowledge the computer resources provided by the Red Española de Supercomputación.

Supporting information for this article is available on the WWW <http://dx.doi.org/10.1002/anie.201405738R2>

Heterogeneous catalysis is commonly governed by surface active sites. Yet, areas just below the surface can also influence catalytic activity, for instance, when fragmentation products of catalytic feeds penetrate inside catalysts. In particular, H absorbed below the surface is required for certain hydrogenation reactions on metals. Herein, we show that sufficient concentration of subsurface hydrogen, H^{sub} , may either increase or decrease significantly the bond energy and the reactivity of the adsorbed hydrogen, H^{ad} , depending on the metal. We predict a representative reaction, ethyl hydrogenation, to speed up on Pd and Pt, but to slow down on Ni and Rh in the presence of H^{sub} , especially on metal nanoparticles. The identified effects of subsurface H on surface reactivity are indispensable for atomistic understanding of hydrogenation processes on transition metals and interactions of hydrogen with metals in general.

For a long time scientists have been studying interaction of hydrogen with transition metals, in particular with Pd. The latter is highly permeable for H and widely used as a hydrogenation catalyst.^[1,2] Despite strong research efforts, it is still controversially discussed in which way H^{sub} atoms absorbed just beneath the top metal layer affect surface reactions. For instance, it is uncertain whether H^{sub} species directly participate in hydrogenation of alkyls on Pd, as also discussed for Ni catalysts.^[3,4] As a touchstone reaction we have chosen alkyl to alkane hydrogenation step, which on Pd catalysts is known to be critically affected by the H^{sub} content.^[5-7] (See also our experimental data in Supporting Information (SI) and in Figure S1.) Importantly, hydrogenation activity of Pd is qualitatively different on single-crystal and nanoparticle (NP) samples.^[6] Thus, to account for a part of the complexity of the subsurface chemistry^[8] and involvement of H^{sub} in the hydrogenation on metal catalysts we go beyond the consideration of only single-crystal surfaces and explore NP models as well. After an in-depth analysis of the processes on Pd we critically compare it with three other transition metals, Pt, Ni and Rh, whose bulk or NP forms were experimentally shown to absorb H.^[4,9]

Our density-functional calculations of Pd catalysts are performed for Pd(111) extended (slab) and unsupported Pd₇₉ NP models with different arrangements and concentrations of H atoms (Figure 1a). Note that bare Pd NPs of a similar size sufficiently accurately mimic the NPs deposited on inert metal-oxides.^[10] We consider the reactivity of terrace sites on {111} facets of the Pd₇₉ NP, which is representative for larger Pd NPs commonly employed in catalytic experiments.^[11] Edge sites are not discussed here since we did not find them to be more active than the terrace sites in the reaction under scrutiny. Theoretical studies reveal that H^{sub} is bound weaker than H^{ad} on Pd^[12] and other transition metals,^[13] implying that at equilibrium conditions H occupies subsurface positions only after filling most of the surface positions.^[5,12,14] In some papers the effect of the H^{ad} atoms on the H^{sub} was considered for

transition metal slabs,^[15] while the influence of H^{sub} on H^{ad} reactivity analyzed in the present paper was not explored in due detail. Thus, for both Pd₇₉ NP and Pd(111) slab different hydrogen contents were represented via three types of models: (i) *low-coverage* models with just one adsorbed H^{ad} atom, $H^{ad}_1H^{sub}_0/Pd(NP)$ and $H^{ad}_1H^{sub}_0/Pd(111)$; (ii) *surface-saturated*^[16] models, $H^{ad}_{78}H^{sub}_0/Pd(NP)$ and $H^{ad}_7H^{sub}_0/Pd(111)$; and (iii) *subsurface-saturated* models, $H^{ad}_{78}H^{sub}_{24}/Pd(NP)$ and $H^{ad}_7H^{sub}_9/Pd(111)$. High exposure of Pd to H₂ under experimental hydrogenation conditions^[Fehler! Textmarke nicht definiert. 5] corresponds to the regimes (ii) or (iii). We study ethyl hydrogenation to ethane, $C_2H_5 + H \rightarrow C_2H_6$, (Figure S6) as a representative surface reaction because alkyl hydrogenation on Pd was observed to be particularly sensitive to the presence of H^{sub} (see SI and Figure S1); our benchmark calculations of butyl hydrogenation on Pd NPs revealed very similar trends in the reactivity (see Table 1). Note, however, that for the examined reaction the surface concentration of the alkyl intermediate hardly depends on the concentration of the H^{sub} species (see SI).

The hydrogenation of ethyl is exothermic by 50–140 kJ mol⁻¹ (Table 1) for all catalyst models addressed, implying that only kinetic aspects need to be investigated in depth. We first examined possible reaction paths of ethyl recombination directly with H^{sub} atom (see Figure S2). However, the attacking H^{sub} emerging from the subsurface area of Pd was inevitably stabilized on the surface and converted to H^{ad} , which subsequently acted as a reactant, similarly to methyl hydrogenation on Ni(111).^[3,4] Therefore, in the following only the attack of alkyl species by a surface H^{ad} atom is discussed.

Results in Figure 1 predict that increasing the hydrogen content should accelerate the reaction on Pd NPs as well as on the Pd(111) single-crystal surface. As one moves from the bare NP with just one H^{ad} to the *surface-saturated* NP, the Gibbs activation energy of hydrogenation decreases by 19 kJ mol⁻¹ (Table 1). This corresponds to a three orders of magnitude higher hydrogenation rate at 298 K. The activation barriers for the *low-coverage* and *surface-saturated* single-crystal models agree within 2 kJ mol⁻¹ with those for the corresponding NP models. This observation corroborates the suitability of the employed NP models to represent bigger Pd NPs studied experimentally.

The prominent difference between NPs and single crystals becomes evident when H is introduced into subsurface region of Pd. For the *subsurface-saturated* NP it causes further strong reduction of the Gibbs activation energy by 24 kJ mol⁻¹ (Table 1). Such barrier lowering should increase the reaction rate by four orders of magnitude compared to the *surface-saturated* NP without H^{sub} . At the same time, the addition of H^{sub} atoms to *surface-saturated* single crystal decreases the barrier by only ~5 kJ mol⁻¹ and accelerates the reaction

tenfold. Hence, we conclude that dramatically accelerated hydrogenation on Pd can be achieved via the synergy of high H^{sub} content and catalyst nanostructuring.^[17]

In order to further evaluate the contributions to the barrier lowering by various H^{ad} and H^{sub} atoms surrounding the reacting species, we considered two more models derived from the most reactive *subsurface-saturated* NP model $H^{ad}_{78}H^{sub}_{24}/Pd(NP)$. First, the most distant H^{ad} and H^{sub} atoms were removed from the $\{111\}$ NP facet that accommodates ethyl reactant, giving $H^{ad}_{38}H^{sub}_{12}/Pd(NP)$ model. Subsequent removal of H atoms most distant from the reaction site results in the model $H^{ad}_{23}H^{sub}_3/Pd(NP)$ (see Figure S3). For the $H^{ad}_{38}H^{sub}_{12}/Pd(NP)$ model, the Gibbs activation barrier of the hydrogenation is 9 kJ mol^{-1} , close to that of the *subsurface-saturated* NP containing about twice as many H^{ad} and H^{sub} atoms. The model with only three H^{sub} atoms located below the reaction site, $H^{ad}_{23}H^{sub}_3/Pd(NP)$, features a barrier height of 28 kJ mol^{-1} , the same as on the *surface-saturated* NP without any H^{sub} atoms. Thus, solely the H^{sub} atoms right beneath the hydrogenation sites on Pd NP are likely insufficient to notably lower the barrier. Rather, the effect of the overall concentration of H^{sub} on the barrier height appears to be gradual. Indeed, the Pd NPs with increasing number of H^{sub} atoms, $H^{ad}_{78}H^{sub}_0 \rightarrow H^{ad}_{23}H^{sub}_3 \rightarrow H^{ad}_{38}H^{sub}_{12} \rightarrow H^{ad}_{78}H^{sub}_{24}$ exhibit decreasing activation barriers $29 \rightarrow 28 \rightarrow 9 \rightarrow 5 \text{ kJ mol}^{-1}$. A similar, but much weaker effect could also be seen on Pd(111) models: the barrier drops from 31 to 26 kJ mol^{-1} while switching from *surface-saturated* to *subsurface-saturated* single-crystal model. Doubling the H^{sub} concentration in the *subsurface-saturated* single-crystal model (by filling the second subsurface layer) further decreases the Gibbs activation barrier from 26 to 18 kJ mol^{-1} . In line with the experimental observations (Figure S1 and the second paragraph in SI), this finding suggests that Pd(111) single-crystal can be as active as Pd NPs in hydrogenation of alkyls, but only at rather high concentration of H^{sub} , which may be difficult to maintain in steady state reaction regime.

What are the fundamental reasons for the enhanced hydrogenation activity of Pd NPs in the presence of H^{sub} species and why is the activation less efficient on the extended Pd(111) surface? To answer these questions, we analyze the energy contributions that determine the barrier heights. From the binding energy of ethyl + H considered as the initial state of the process, IS, E_b^{IS} (Table 1), one notices that the increase in the H content gradually destabilizes the IS structures on NP and, to a lesser extent, on single-crystal models. The transition state (TS) destabilization caused by H^{sub} atoms is not so strong, as seen from its binding energy, E_b^{TS} (Table 1). The different destabilization of the IS and TS structures by H^{sub} atoms deter-

mines the activation energies, which are lowered by 24 kJ mol⁻¹ on the NP and by 5 kJ mol⁻¹ on the single crystal when changing from *surface-saturated* to *subsurface-saturated* model.

The data presented in Table 1 suggest that the binding energy of an attacking H^{ad} (without co-adsorbed ethyl) is a descriptor of the surface hydrogenation reactivity. The adsorption energies of the probe atom H, E_b(H), correlate with the activation energies of ethyl hydrogenation (Figure 2): lowering of E_b(H) is accompanied by a decrease of the Gibbs activation barrier by almost the same amount. Thus, a destabilization of H^{ad} by H^{sub}, consistent with experimental observations,^[18] appears to be the main reason for the activation of Pd catalysts by subsurface H, which is particularly strong on Pd NPs.

Examining the electronic structure of Pd with varying number of H^{ad} and H^{sub} atoms is the key to understanding the origin of the weakened adsorption of H atoms and their enhanced reactivity. Two effects are manifested in densities of states (DOS) projected on H *s* and Pd *d* states of atoms forming three-fold hollow hydrogenation sites H^{ad}Pd₃ (Figures 3, S3, S4). First, a shift of the Pd *4d* states to lower energies with increasing H content notably reduces the number of states at the Fermi level. The magnitude of these H-induced DOS shifts, ca. 0.3 eV, is comparable to differences between *d*-band centers of such distinct metals as Cu and Pt,^[19] explaining the dramatic change in catalytic properties of Pd upon saturation with H. The second effect is related to the DOS of the *subsurface-saturated* NP model, for which the lowest hydrogenation activation energy is computed. The H *s*-projected DOS reveals a small feature just below the Fermi level corresponding to a partial occupation of the antibonding H^{ad}-Pd₃ states (see asterisks in Figure 3). The latter, in line with the reactivity analysis of different late transition metals with respect to H,^[20] results in a notably weaker interaction between H^{ad} and Pd. Both effects on DOS plots described above are significantly stronger for NPs than for single-crystal models. Filling of subsurface sites by H atoms in the *subsurface-saturated* single crystal does not lead to any noticeable occupation of the antibonding H^{ad}-Pd states, consistent with the substantial ethyl hydrogenation barrier of 26 kJ mol⁻¹. Thus, high sensitivity of NPs to changes in electronic structure upon interaction with hydrogen is crucial for activation of Pd by H^{sub}. This explains why both subsurface hydrogen and nanostructuring of Pd catalysts are necessary for the high observed steady state hydrogenation activity. Note that changes in geometric structure of Pd catalysts induced by H^{sub} cannot explain the increase in the hydrogenation activity (see SI).

Having analyzed the interplay between H^{sub} content and hydrogenation catalytic activity for Pd, we explored to what extent the trends identified for Pd are inherent to transition metals in general. To this end we investigated other catalytically relevant metals – Pt, Ni and Rh –

using the same models as for Pd and calculated binding energies of adsorbed hydrogen, $E_b(\text{H})$, as a descriptor of the hydrogenating activity, and its dependence on the content of subsurface hydrogen. For one of the metals, Ni, we also calculated hydrogenation rates, Figure 1b, which are shown to be related to $E_b(\text{H})$, as discussed above for Pd.

The results collected in Table 2 suggest that Pt behaves similarly to Pd – the binding energy of H^{ad} is decreased in magnitude from -49 kJ mol^{-1} on the *low-coverage* Pt NP to -13 kJ mol^{-1} on the *subsurface-saturated* NP. Again this sharp weakening of H^{ad} binding is related to changes in the electronic structure and partial occupation of antibonding H-Pt states (Figure S5). On the single-crystal Pt(111) surface the weakening of H^{ad} binding is much more modest, only to -30 kJ mol^{-1} for the *subsurface-saturated* model.

In contrast, the binding nature of hydrogen to Ni and Rh appears to be remarkably different from that to Pd and Pt due to distinctively polar H-Ni and H-Rh bonds with significantly larger electron density accumulated on hydrogen and concomitantly increased positive charge on metal atoms (Table 2). Addition of H^{sub} to hydrogen-loaded Ni and Rh systems is predicted to lead to further electron depletion from the surface metal atoms and increase their electrostatic attraction to the adsorbed (noticeably negatively charged) H^{ad} atoms. Thus, in striking variance with Pd and Pt, the presence of H^{sub} in Ni and Rh makes H^{ad} atoms more strongly bound to the metal. Keeping in mind our findings for Pd, one could expect that this stabilization results in decreased activity of H^{ad} in the presence of H^{sub} . Indeed, we calculated (Table 1, Figure 1b) that on Ni nanoparticles H^{sub} slows down ethyl hydrogenation by three orders of magnitude.

In summary, we determined two mechanisms by which subsurface H may affect the activity of transition metals, in particular, in hydrogenation reactions. On Pd and Pt subsurface H destabilizes adsorbed H via changing the electronic structure of metals, causing occupation of anti-bonding H^{ad} -Pd or H^{ad} -Pt electronic states. This effect is stronger on metal NPs than on single crystals and is sufficient to accelerate alkyl hydrogenation by several orders of magnitude on Pd NPs. Moreover, the hydrogenation rate is found to increase gradually with increasing H^{sub} content even at a distance from the reaction site. Thus, the structure of active sites alone (similar in NPs and single crystals) does not yet determine the reactivity. Our findings help to clarify a long-standing puzzle why both subsurface hydrogen and nanostructuring of Pd catalysts are necessary for the observed high steady-state olefin hydrogenation activity. Importantly, the outlined mechanism of H^{ad} activation is inherent to H-Pd and H-Pt interactions and, thus, should affect various hydrogenation (and dehydrogenation) reactions on these catalysts. In a very remarkable contrast, on Ni and Rh we have found another

mechanism of interplay between adsorbed and subsurface H, which leads to the stabilization of adsorbed H. This behavior is due to the more polar character of H-Ni and H-Rh bonds, which leads to increased positive charge of surface metal atoms due to the presence of H^{sub} and consequently stronger electrostatic attraction of (negatively charged) H^{ad} to the surface. Notable deactivation of adsorbed H by subsurface H on Ni NPs is manifested by decreased reaction rates for ethyl hydrogenation. At the same time, desorption of surface H should be also hindered by subsurface H on Ni and Rh, which may be beneficial for certain reactions. From practical point of view, the discussed mechanisms of destabilization or stabilization of adsorbed H by adsorbed H may be used to tune catalytic activity of transition metals.

Keywords: density functional calculations · heterogeneous catalysis · hydrogenation · nanoparticles · surface chemistry

Table 1: Calculated data for ethyl hydrogenation catalyzed by Pd and Ni. Rate constant, activation and reaction Gibbs free energies at temperature $T = 298$ K (k_{298} , ΔG_{298}^\ddagger and ΔG_{298} , respectively), binding energies (E_b) of atom H^{ad} as well as those of initial state (IS) and transition state (TS) structures on various forms of the catalysts.^[a]

Model ^[b]	k_{298} ^[c]	ΔG_{298}^\ddagger	ΔG_{298}	$E_b^{IS}(C_2H_5+H)$	$E_b^{TS}(C_2H_5+H)$	$E_b(H)$
	s^{-1}	$kJ\ mol^{-1}$	$kJ\ mol^{-1}$	$kJ\ mol^{-1}$	$kJ\ mol^{-1}$	$kJ\ mol^{-1}$
Pd nanoparticle						
<i>low-coverage</i>	2×10^4	48	-51	-219	-165	-61
<i>surface-saturated</i> ^[d]	5×10^7	29	-100	-178	-133	-51
	(2×10^6)	(37)	(-106)			
<i>subsurface-saturated</i> ^[d]	8×10^{11}	5	-142	-134	-119	-15
	(7×10^9)	(17)	(-142)			
Pd single crystal						
<i>low-coverage</i>	2×10^4	48	-58	-205	-155	-56
<i>surface-saturated</i>	2×10^7	31	-103	-174	-133	-43
<i>subsurface-saturated</i>	2×10^8	26	-126	-152	-115	-34
Ni nanoparticle						
<i>surface-saturated</i>	1×10^7	33	-105	-176	-132	-66
<i>subsurface-saturated</i>	9×10^3	51	-52	-207	-149	-69
Ni single crystal						
<i>surface-saturated</i>	1×10^{10}	16	-137	-147	-122	-51
<i>subsurface-saturated</i>	7×10^9	17	-126	-165	-133	-60

[a] E_b is the binding energy to the metal substrate of either the co-adsorbed species C_2H_5+H (with respect to the energy of free $C_2H_5+\frac{1}{2} H_2$) or the atom H^{ad} involved in the hydrogenation (calculated without co-adsorbed ethyl, with respect to the energy of $\frac{1}{2} H_2$).

[b] See Figure 1.

[c] $k_T = (k_B T/h) \times \exp(-\Delta G_T^\ddagger / RT)$, where k_B , h and R are Boltzmann, Planck and ideal gas constants, respectively.

[d] In parentheses, the data for butyl hydrogenation are shown.

Table 2: Results for nanoparticle and (111) single-crystal models of transition metals interacting with a different number of hydrogen atoms. Binding energies of adsorbed hydrogen atoms, $E_b(\text{H})$, and calculated Bader charges, q , of selected atoms.

Model ^[a]	$E_b(\text{H})$, ^[b] kJ mol ⁻¹				$q(\text{H})$, ^[c] e				$q(\text{M})$, ^[d] e			
	Ni	Rh	Pd	Pt	Ni	Rh	Pd	Pt	Ni	Rh	Pd	Pt
Nanoparticle												
<i>low-coverage</i>	-63	-49	-61	-49	-0.27	-0.21	-0.11	-0.04	0.10	0.07	0.03	0.02
<i>surface-saturated</i>	-66	-37	-51	-47	-0.22	-0.16	-0.09	-0.02	0.17	0.11	0.08	0.01
<i>subsurface-saturated</i>	-69	-66	-15	-13	-0.28	-0.20	-0.11	-0.04	0.29	0.19	0.11	0.05
					(-0.27)	(-0.15)	(-0.08)	(0.00)				
Single crystal												
<i>low-coverage</i>	-54	-56	-56	-47	-0.28	-0.22	-0.13	-0.08	0.07	0.03	0.03	-0.02
<i>surface-saturated</i>	-51	-47	-43	-39	-0.25	-0.20	-0.12	-0.05	0.19	0.13	0.09	0.03
<i>subsurface-saturated</i>	-60	-52	-34	-30	-0.27	-0.20	-0.13	-0.06	0.27	0.15	0.12	0.01
					(-0.29)	(-0.17)	(-0.11)	(-0.01)				

[a] See models depicted in Figure 1.

[b] $E_b(\text{H})$ is the binding (adsorption) energy of the H^{ad} atom involved in the hydrogenation (calculated without co-adsorbed ethyl species) vs. free $\frac{1}{2} \text{H}_2$.

[c] Average charges of all adsorbed atoms H^{ad} , or, in parentheses, of all subsurface atoms H^{sub} .

[d] Average charges of the three metal atoms M, to which the attacking atom H^{ad} is coordinated.

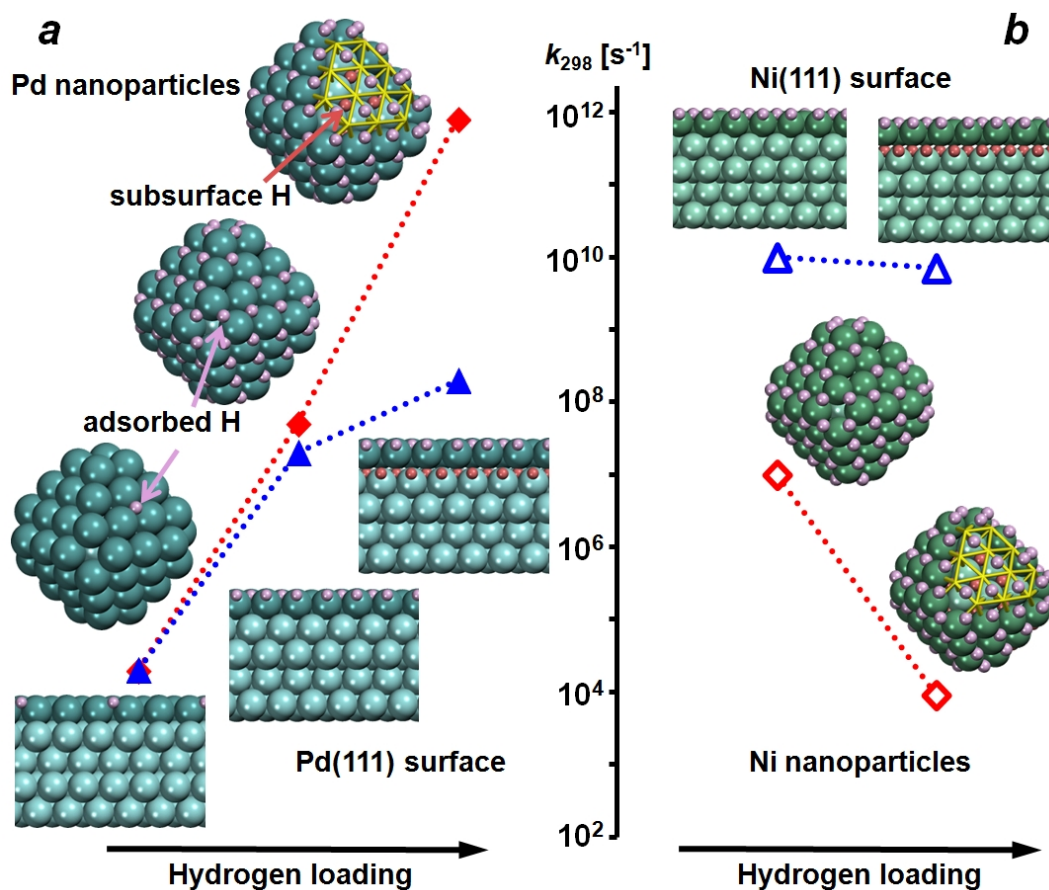


Figure 1: Calculated rate constant k_{298} of ethyl hydrogenation on Pd (a) and Ni (b) at 298 K as a function of hydrogen loading and nanostructuring of the catalyst. Data for metal nanoparticles (red diamonds) and (111) single-crystals (blue triangles) are shown together with the sketches of the models.

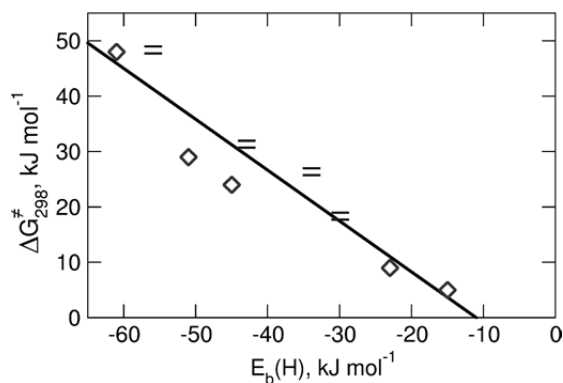


Figure 2: Correlation of activation barriers with adsorption energies of hydrogen. Activation Gibbs free energies of ethyl hydrogenation, $\Delta G^{\ddagger}_{298}$, as a function of H binding energies in IS, $E_b(\text{H})$, calculated on Pd NP (\diamond) and Pd(111) single crystal (=) models.

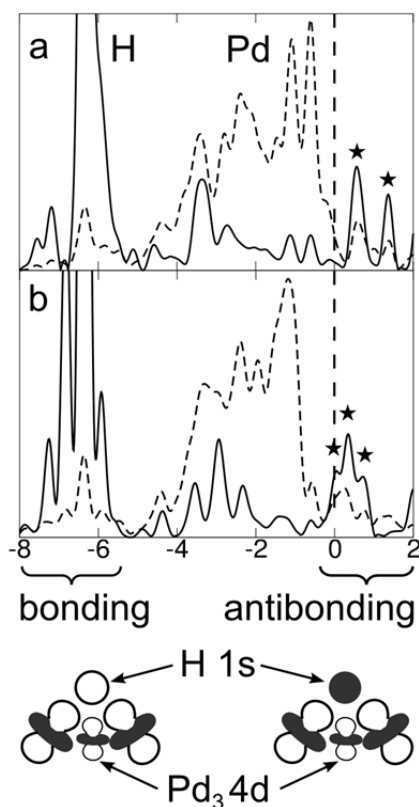


Figure 3: Dependence of the electronic structure of nanoparticulate Pd-H systems on the hydrogen content: *a* – Pd₇₉ NP saturated with adsorbed hydrogen H^{ad}, *b* – Pd₇₉ NP saturated with both adsorbed H^{ad} and subsurface H^{sub} hydrogen (see Figure 1a). The density of states (DOS) projected on: solid line – *s* states of the reacting H^{ad} atom ($\times 50$); dashed line – *d* states of the atoms forming the hollow site Pd₃, where the atom H^{ad} is located. DOS is given in arbitrary units, with respect to the Fermi energy $\varepsilon_F = 0$ eV. The H-Pd₃ antibonding states (marked by asterisks) approach the Fermi level with increasing H content, resulting in their partial occupation in *subsurface-saturated* NP (panel *b*).

References

- [1] *Handbook of Heterogeneous Catalysis* (Eds.: G. Ertl, H. Knözinger, J. Weitkamp), Wiley-VCH, Weinheim, **1997**.
- [2] D. Teschner, J. Borsodi, A. Wootsch, Z. Révay, M. Hävecker, A. Knop-Gericke, S. D. Jackson, R. Schlögl, *Science* **2008**, *320*, 86–89.
- [3] a) A. D. Johnson, S. P. Daley, A. L. Utz, S. T. Ceyer, *Science* **1992**, *257*, 223–225; b) G. Henkelman, A. Arnaldsson, H. Jónsson, *J. Chem. Phys.* **2006**, *124*, 044706.
- [4] S. T. Ceyer, *Acc. Chem. Res.* **2001**, *34*, 737–744.
- [5] M. Wilde, K. Fukutani, W. Ludwig, B. Brandt, J.-H. Fischer, S. Schauerer, H.-J. Freund, *Angew. Chem. Int. Ed.* **2008**, *47*, 9289–9293; *Angew. Chem.* **2008**, *120*, 9430–9434.
- [6] A. M. Doyle, S. K. Shaikhutdinov, S. D. Jackson, H.-J. Freund, *Angew. Chem. Int. Ed.* **2003**, *42*, 5240–5243; *Angew. Chem.* **2003**, *115*, 5398–5401.
- [7] a) W. Ludwig, A. Savara, K.-H. Dostert, S. Schauerer, *J. Catal.* **2011**, *284*, 148–156; b) W. Ludwig, A. Savara, S. Schauerer, H.-J. Freund, *ChemPhysChem* **2010**, *11*, 2319–2322.
- [8] M. Armbrüster, M. Behrens, F. Cinquini, K. Föttinger, Y. Grin, A. Haghofer, B. Klötzer, A. Knop-Gericke, H. Lorenz, A. Ota, S. Penner, J. Prinz, C. Rameshan, Z. Révay, D. Rosenthal, G. Rupprechter, P. Sautet, R. Schlögl, L. Shao, L. Szentmiklósi, D. Teschner, D. Torres, R. Wagner, R. Widmer, G. Wowsnick, *ChemCatChem* **2012**, *4*, 1048–1063.
- [9] a) M. Yamauchi, H. Kobayashi, H. Kitagawa, *ChemPhysChem* **2009**, *10*, 2566–2576; b) H. Kobayashi, H. Morita, M. Yamauchi, R. Ikeda, H. Kitagawa, Y. Kubota, K. Kato, M. Takata, *J. Am. Chem. Soc.* **2011**, *133*, 11034–11037.
- [10] a) S. M. Kozlov, H. A. Aleksandrov, J. Goniakowski, K. M. Neyman, *J. Chem. Phys.* **2013**, *139*, 084701; b) S. M. Kozlov, H. A. Aleksandrov, K. M. Neyman, *J. Phys. Chem. C* **2014**, *118*, 15242–15250.
- [11] I. V. Yudanov, R. Sahnoun, K. M. Neyman, N. Rösch, *J. Chem. Phys.* **2002**, *117*, 9887–9896.
- [12] H. A. Aleksandrov, F. Viñes, W. Ludwig, S. Schauerer, K. M. Neyman, *Chem. - Eur. J.* **2013**, *19*, 1335–1345.
- [13] P. Ferrin, S. Kandoi, A. U. Nielekar, M. Mavrikakis, *Surf. Sci.* **2012**, *606*, 679–689.
- [14] K. M. Neyman, S. Schauerer, *Angew. Chem. Int. Ed.* **2010**, *49*, 4743–4746; *Angew. Chem.* **2010**, *122*, 4851–4854.
- [15] a) J. Greeley, M. Mavrikakis, *Surf. Sci.* **2003**, *540*, 215–229; b) J. Greeley, W. P. Krekelberg, M. Mavrikakis, *Angew. Chem. Int. Ed.* **2004**, *43*, 4296–4300; *Angew. Chem.* **2004**, *116*, 4396–4400.
- [16] Leaving vacant only surface sites required for modelling adsorption and hydrogenation of olefin reactant.
- [17] Not only the activation barriers can be affected by co-adsorbed species, such as H^{sub} or hydrocarbons. Also, the binding energies of the intermediates can be influenced, which might modify the concentrations and the relative distribution of all surface species in a complex way. Description of this complicated interplay using extensive electronic structure and kinetic Monte-Carlo calculations is beyond the scope of this communication.
- [18] E. C. H. Sykes, L. C. Fernández-Torres, S. U. Nanayakkara, B. A. Mantooth, R. M. Nevin, P. S. Weiss, *PNAS* **2005**, *102*, 17907–17911.
- [19] A. Ruban, B. Hammer, P. Stoltze, H. L. Skriver, J. K. Nørskov, *J. Mol. Catal. A* **1997**, *115*, 421–429.
- [20] B. Hammer, J. K. Nørskov, *Nature* **1995**, *376*, 238–240.